R.F. SPECTRUM OF THERMAL NOISE AND FREQUENCY STABILITY OF A MICROWAVE CAVITY-OSCILLATOR

B. Villeneuve, P. Tremblay, A. Michaud and M. Têtu

Laboratoire de recherche sur les oscillateurs et systèmes
Département de génie électrique, Université Laval
Québec G1K 7P4 - Canada

ABSTRACT

The spectral distribution of the thermal noise within a microwave cavity equipped with an external feedback loop has been calculated and measured. An equivalent electrical model is established from which the noise spectral density can be calculated at any port in the system. The effect of the gain and phase of the loop on the spectral distribution is measured with a spectrum analyzer through an heterodyne technique. Comparison with theoretical calculations shows good agreement. Preliminary meaurements of the short term frequency stability of the system when operated as a microwave cavity-oscillator show a predominant flicker frequency noise. The F.M. noise close to carrier is measured and related to time domain measurements.

INTRODUCTION

The quality factor, Q, of a microwave cavity can be varied easily over a wide range if it is equipped with an external feedback loop having a variable gain and a variable total phase shift (1). The Q factor can be reduced or increased and the system becomes an oscillator when its value reaches infinity. Microwave cavities using such artificially enhanced Q factor are encountered in atomic frequency standard technology where small size devices are built using this approach (2). With this type of standards, it has been observed through frequency stability measurements that the effect of thermal noise within the cavity varies greatly with the parameters of the external loop (3). We present in this paper a theoretical evaluation of the spectral distribution of this thermal noise for various operating conditions and compare the calculated results to measured data. We give also preliminary results on the study of frequency stability and F.M. noise for this type of system when operated as a cavity-oscillator.

THERMAL NOISE

Radio-electrical model

The considered microwave cavity and its feedback loop (or the microwave cavity-oscillator) can be represented schematically through Fig. 1. Power is coupled in and out of the cavity with coupling coefficient β_2 and β_1 respectively. The external loop consists of a commercial low noise GaAs FET amplifier, a variable attenuator, a variable phase shifter and two isolators, one at each end of the loop. The output signal is observed through an A.M. heterodyne receiver. In this set up discrete elements are used in order to evaluate separately their contribution to the behavior of the whole system.

A radio-electrical model equivalent to the cavity and its loop is given in Fig. 2. We consider in this relatively simple model only the noise sources E_c from the cavity (black body radiation), E_1 and E_2 from the dummy loads of the isolators, E_a from the low noise amplifier and E_r from the receiver. The Ψ_i's represent the phase shifts between the loop elements at frequency f_o and the other symbols have the usual meanings.

In order to find an expression for the power spectral density of the load voltage, we first evaluate the transfer functions of each independent noise source, which are assumed of thermal nature. We find that the cavity Q and resonant frequency are modified in the following manner:

$$Q'_c = \frac{Q_o}{1+\beta_1+\beta_2-2G\sqrt{\beta_1\beta_2}\cos\psi}$$

and

$$f'_o \simeq f_o(1 + \frac{G\sqrt{\beta_1\beta_2}}{Q_o}\sin\psi), \qquad (1)$$

where Q_o is the unloaded cavity Q, G is the total loop voltage gain and ψ is the total loop phase shift, which are:

$$G = G_a G_s G_L \quad \text{and} \quad \psi = \sum_{i=1}^{7}\psi_i + \psi_p.$$

The power spectral density delivered to the load is defined as:

$$P_o(f) = \frac{S_{V_o}(f)}{Z_o}.$$

The complete calculation gives:

$$P_o(f) = kG_r^2G_a^2G_s^2\left[\frac{T_r}{G_a^2G_s^2} + \right.$$

$$\left. + \frac{[(1+\beta_1+\beta_2)^2+(Q_o\Delta)^2]T_a+4\beta_1(\theta_c+\beta_1\theta_1+\beta_2\theta_2)}{(1+\beta_1+\beta_2-2G\sqrt{\beta_1\beta_2}\cos\psi)^2 + (Q_o\Delta-2G\sqrt{\beta_1\beta_2}\sin\psi)^2}\right], \quad (2)$$

where T_r and T_a are the equivalent noise tempe-
ratures of the receiver and the low noise amplifier
respectively, θ_1, θ_2 and θ_c are the thermodynamic
temperatures of the isolator 1, 2 and the cavity
respectively, and Δ is:

$$\Delta = \frac{f}{f_o} - \frac{f_o}{f} \simeq \frac{2(f - f_o)}{f_o}.$$

Eq. (2) gives the spectral distribution of the
noise at the output of a receiver "looking" at a
system "cavity + feedback loop". The first term is
the contribution from the receiver while the second
term represents the contribution of the noisy ele-
ments within the loop.

Experimental measurements

The power spectral distribution of the thermal
noise generated within the system for various total
loop gain and phase shift is measured directly with
a spectrum analyser (AIL 757) at the I.F. frequency
(30 MHz) of a low noise heterodyne A.M. receiver.
The loop gain, $G(a,p)$, and the loop phase shift,
$\Psi(a,b)$, are manually changed through the use of
micrometer variable attenuator (setting a) and
phase shifter (setting p). Calibration of the
indicator settings is done with a network analyzer
(HP 8410). Figs 3 and 4 give the resulting varia-
tions of the loop gain and phase for the two para-
meters a and p respectively. It is observed that
these do not provide independent control of the
gain and phase, but the information of Figs 3 and 4
allows their precise determination for any settings
of a and p.

Fig. 5a gives the noise power spectral density
for various attenuator settings (loop gain) while
the phase shifter setting was maintained at a fixed
value (total phase shift close to zero). It is
observed that the curves are almost symmetrical
around the resonant frequency of the cavity (6.835
GHz). The height increases rapidly with the loop
gain while the noise floor stays at the same level.
If the loop gain is increased to a value higher
than the maximum one indicated on the figure, the
system starts to oscillate. The output power grows
until the gain of the amplifier compresses and the
total loop gain equals the losses in the cavity and
its coupling elements. The frequency at which the
maximum occurs varies slightly because the total
phase shift of the loop changes with the attenuator
setting as shown in Fig. 3 (see Eq. (1)).

If the attenuator setting is maintained at a
fixed value (a = 2.79) and the phase shifter set-
ting is varied, the noise power spectral density
varies as shown on Fig. 5b. In this figure the
loop phase shift varies from $\simeq 0°$ to 180°. At $\psi \simeq$
0° (p = 5.98) the curve 5 corresponds to curve 1 of
Fig. 5a. For $\psi \simeq 180°$ (p = 3.60) the noise spec-
tral distribution is reduced symmetrically around
the resonant frequency (f_o = 6.835 GHz) of the
cavity. For the other phase settings the distribu-
tions are not symmetrical and a hump appears at a
frequency offset from f_o. It was shown experi-
mentally that oscillation condition can be reached
for a phase shifter setting different from p = 5.98
if the loop gain is sufficiently high.

Theoretical calculations

Theoretical evaluation of Eq. (2) has been per-
formed for various parameter settings of the system
studied. The values of the fixed parameters are
given in Table 1.

Table 1 - Microwave cavity and feedback loop
parameters

k	= Boltzmann constant:	1.381×10^{-23} J/K
β_2	= input coupling coefficient:	0.25
β_1	= output coupling coefficient:	0.25
Q_o	= unloaded cavity quality factor:	25000
f_o	= cavity resonant frequency:	6.835 GHz
G_a	= amplifier voltage gain:	17.48 (24.8dB)
G_s	= power splitter voltage gain:	0.668 (- 3.5dB)
G_R	= receiver voltage gain:	573.5 (55.2dB)
T_a	= amplifier equivalent noise temperature:	190K
T_R	= receiver equivalent noise temperature:	254K
θ_1	= thermodynamic temperature of isolator 1:	290K
θ_2	= thermodynamic temperature of isolator 2:	290K
θ_c	= thermodynamic temperature of the cavity:	290K

For each experimental curve of Figs 5a and 5b, we
need to evaluate the "real" gain and phase of the
loop. Curve 1 of Fig. 5a has been taken at a set-
ting which gives the most symmetrical spectrum we
could get; the loop phase shift is then 0°. The
associated loop gain is adjusted to give the same
peak level than curve 1 of Fig. 5a, and is found to
be 9.45 dB. From the calibration curves, we get:
G = 12 dB and ψ = 37.5°. The loop gain and phase
for the other curves will then be obtained
straightly by taking off 2.55 dB from the "calibra-
ted" gain and 37.5° from the phase. These repre-
sent constant losses and phase shifts associated
with the cavity coupling elements. The resulting
values, and the corresponding plot are shown in
Figs 6a and 6b.

We observe a good agreement between the theore-
tical calculations and experimental data and notice
that, even if the curves are not taken at "round"
values of loop gain and phase, the calibration used
allows an effective evaluation of these variables.

We have shown through a thorough experimental
study that Eq. (2) expresses properly the power
spectral density of the thermal noise generated in
a microwave system consisting of a cavity and a
feedback loop to enhance the cavity Q factor. We
now look at some aspects of the frequency stability
characterization of this system operated as a cavi-
ty-oscillator.

FREQUENCY STABILITY

Time domain measurement

The r.f. spectrum of a highly stable oscillator
is simply related, under certain conditions, to the
spectral density of its phase fluctuations, $S_\phi(f)$
or its short term frequency stability (4). The
short term frequency stability is expressed by the
two sample variance of the mean fractional frequen-
cy fluctuations over an averaging time τ, $\sigma_y^2(\tau)$,
(often called Allan variance).

We have measured the frequency stability of a
microwave cavity-oscillator as considered in the

previous section by beating its output signal to the signal of a rubidium 87 maser and counting the beat signal generated in a A.M. heterodyne receiver (6). The beat frequency was set at 200 kHz and the signal bandpass filtered. The results of the measurement are shown in Fig. 7 as the two sample standard deviation, for various averaging times. This curve shows that:

$$\sigma^2(\tau) \simeq 3 \times 10^{-18}\tau^0 \quad \text{for} \quad 10^{-4}s < \tau < 1 \text{ s}$$

and   (3)

$$\sigma^2(\tau) \simeq 3 \times 10^{-20}\tau^{+2} \quad \text{for} \quad 1 \text{ s} < \tau < 100 \text{ s}.$$

The first type of frequency instabilities (τ^0) is referred to as flicker of frequency noise while the second one (τ^{+2}) is related to frequency drift.

In order to crosscheck the validity of these results we have measured also the frequency stability in the frequency domain.

Frequency domain measurement

The frequency stability is characterized in the frequency domain by the spectral density of the fractional frequency fluctuations, $S_y(f)$ (5). We have measured this spectral density through the method of tight phase locking a reference oscillator (7-8). The result obtained for the frequency range of 1 Hz to 256 Hz is given in Fig. 8. We observe clearly a flicker of frequency noise expressed as:

$$S_y(f) = 4 \times 10^{-18}f^{-1} \quad \text{for} \quad 6 \text{ Hz} < f < 256 \text{ Hz}. \quad (4)$$

If we utilize the translation relation defined in (5), we find that this contribution should give, in a time domain measurement, an Allan variance of $2.7 \times 10^{-18}\tau^0$ which effectively confirm the result given in the previous section.

The results obtained in the frequency domain measurement indicate that the phase noise spectral density should be:

$$S_\phi(f) = \frac{f_o^2}{f^2} S_y(f)$$

$$= 2 \times 10^2 f^{-3} \quad \text{for} \quad 6 \text{ Hz} < f < 256 \text{ Hz}. \quad (5)$$

This behavior is encountered in the study of microwave feedback oscillator using FET amplifiers (9) and is likely to be generated in the amplifier itself.

CONCLUSION and DISCUSSION

We have established a formalism that allows the computation of the thermal noise generated in a system consisting of a microwave cavity equipped with an external feedback loop. We have proved the validity of the model by a thorough experimental study, so the effect of any parameter changes can be predicted with accuracy. This approach can be applied to other types of feedback oscillators.

A measurement set up used to characterize the short term frequency stability of atomic frequency standards has been adapted to study the system operated as a microwave cavity-oscillator. The frequency stability exhibits a τ^0 dependency for time domain measurement or a flicker of frequency noise, f^{-1} dependency, for the spectral density of the fractionnal frequency fluctuations (F.M. noise). More measurements are needed in order to fully characterize the behavior of this system as a microwave oscillator.

References

(1) C. Audoin, "Le maser à hydrogène en régime transitoire", Rev. Phys. Appl., 2, pp. 309-320, 1967.

(2) H.T.M. Wang, "An oscillating compact hydrogen maser", Proc. 34th Ann. Symp. on Frequency Control, pp. 364-369, 1980.

(3) M. Têtu, P. Tremblay, P. Lesage, P. Petit, "Experimental study of the frequency stability of a maser oscillator operated with an external feedback loop", IEEE Trans. Instrum. Meas., 32, pp. 410-413, 1983.

(4) J.H. Shoaf, D. Halford, A.S. Risley, "Frequency stability specifications and measurement: high frequency and microwave signals", NBS Technical Note 632, January 1973.

(5) J.A. Barnes et al., "Characterization of frequency stability", IEEE Trans. Instrum. Meas., 20, pp. 105-120, 1971.

(6) M. Têtu, G. Busca, J. Vanier, "Short-term frequency stability of the Rb^{87} Maser", IEEE Trans. Instrum. Meas., 22, pp. 250-257, 1973.

(7) B.E. Blair, Ed., "Time and Frequency: Theory and Fundamentals", Washington, D.C., U.S. Dept. Commerce, NBS Mon. 140, 1974, Ch. 8.

(8) M. Têtu, R. Brousseau, J. Vanier, "Frequency-Domain measurement of the frequency stability of a maser oscillator", IEEE Trans. Instr. Meas., 29, pp. 94-97, 1980.

(9) R.A. Pucel, J. Curtis, "Near-carrier noise in FET oscillators", 1983 IEEE MTT-S Int. Microwave Symp. Digest, pp. 282-284.
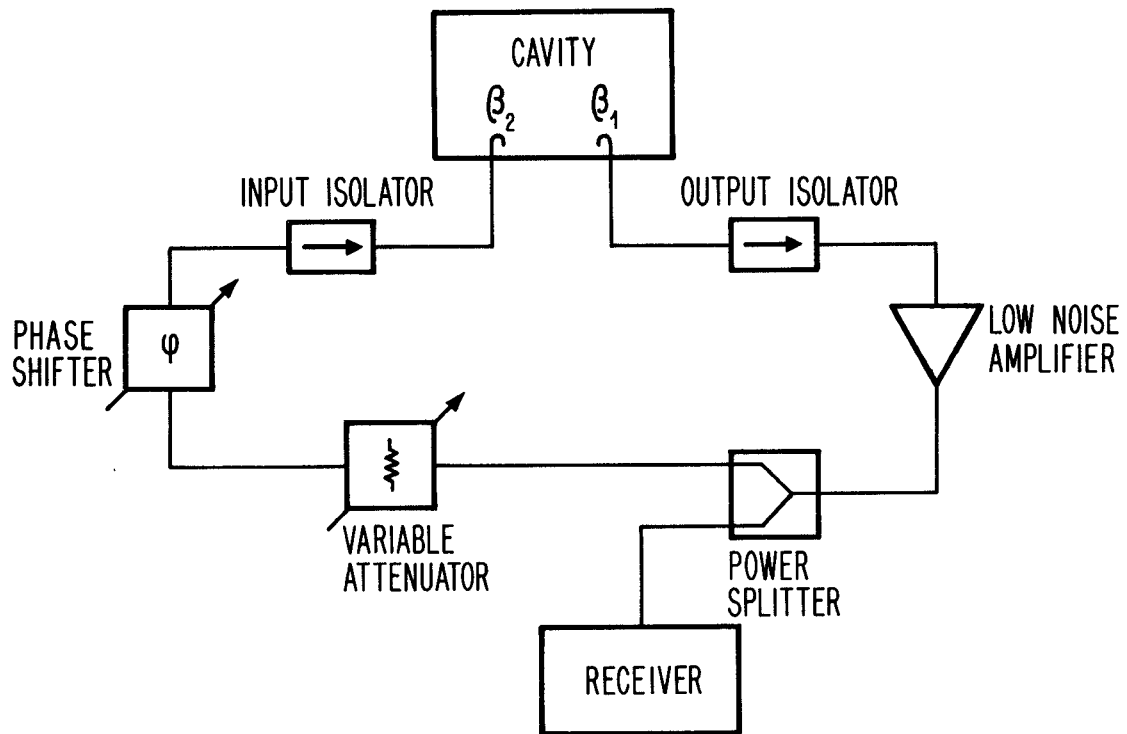
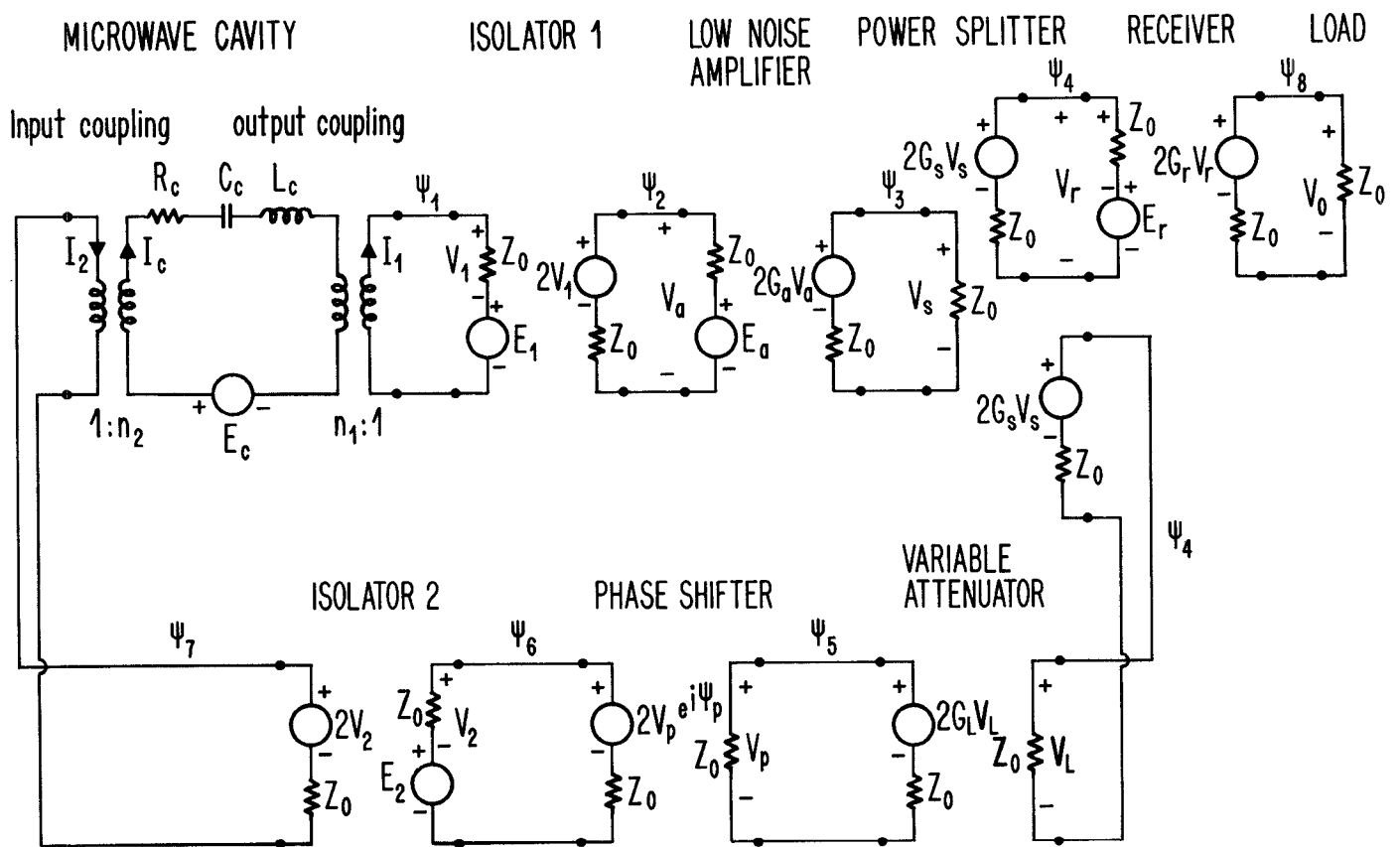Figure 1 – Schematic diagram of a microwave cavity equipped with an external feedback loop.

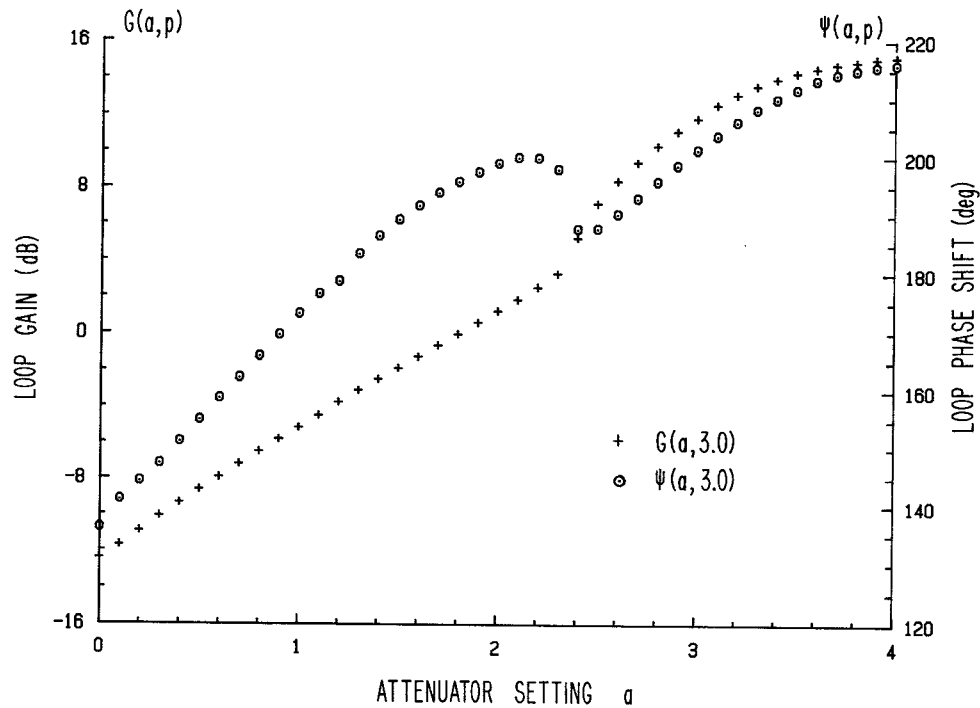Figure 2 – Radio-electrical model of the cavity and its feedback loop.

Figure 3 — Calibration curves of the loop gain and phase shift as functions of the attenuator setting. For each curve the phase shifter setting was fixed at p = 3.00.
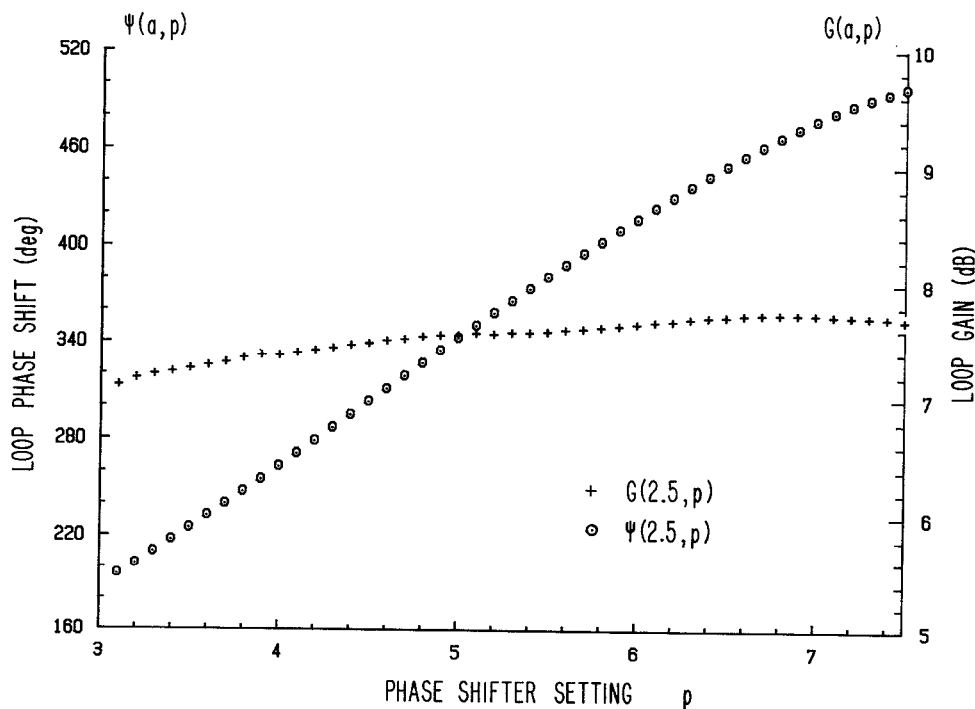

Figure 4 — Calibration curves of the loop phase shift and gain as functions of the phase shifter setting. For each curve the attenuator setting was fixed at a = 2.50.

Figure 5 - Power spectral density of thermal noise delivered to a load as a function of frequency offset from the cavity resonant frequency, f_o:

a) for various attenuator settings: 1) a = 2.79, 2) a = 2.70, 3) a = 2.55, 4) a = 2.30 and a constant phase shifter setting: p = 5.98;

b) for various phase shifter settings: 5) p = 5.98, 6) p = 5.70, 7) p = 5.40, 8) p = 5.10, 9) p = 4.80, 10) p = 4.20, 11) p = 3.60 and a constant attenuator setting: a = 2.79.
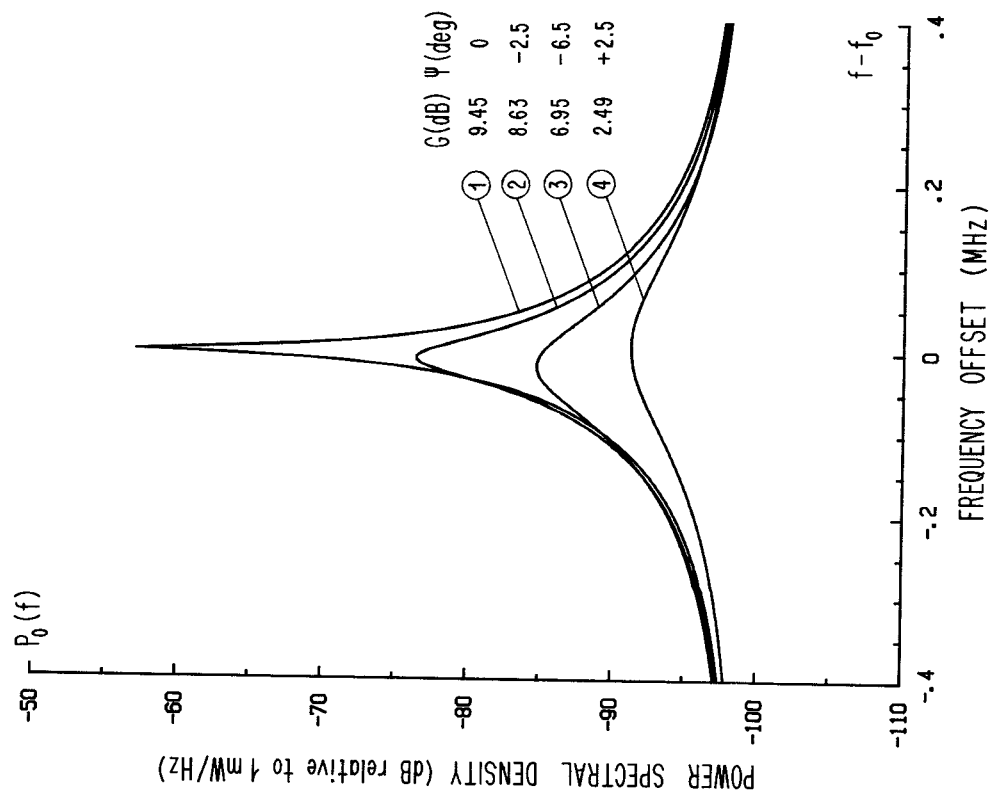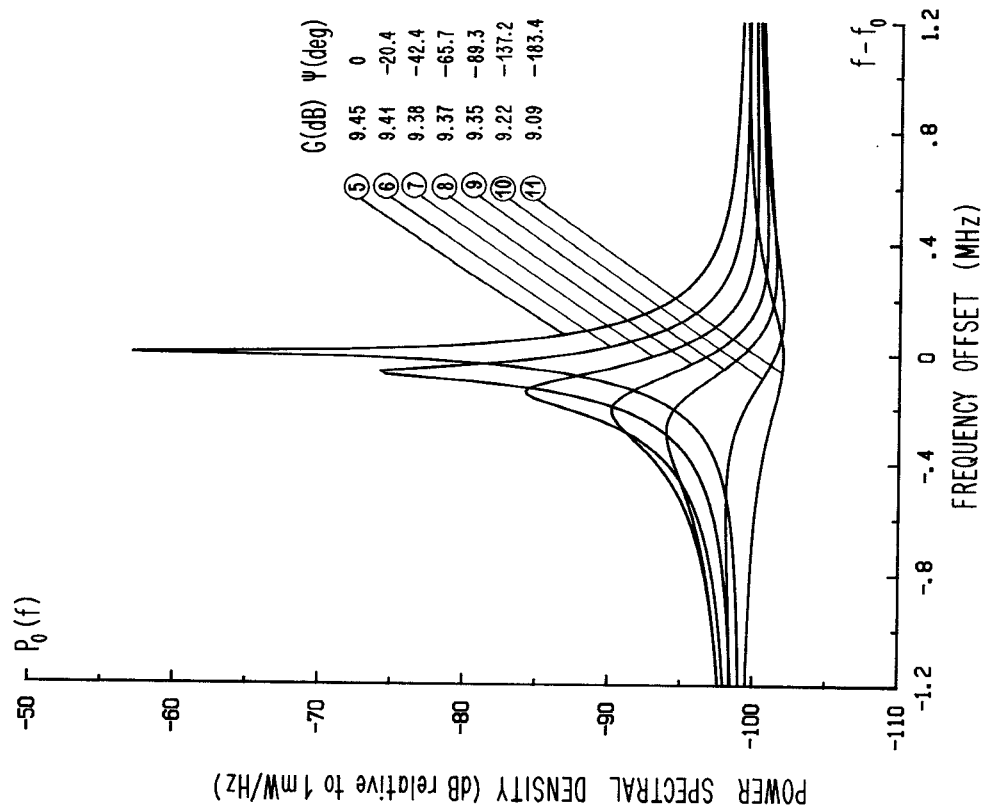
Figure 6 – Theoretical evaluation of the power spectral density of the thermal noise:

a) for parameter settings equivalent to Fig. 5a;   b) for parameter settings equivalent to Fig. 5b.
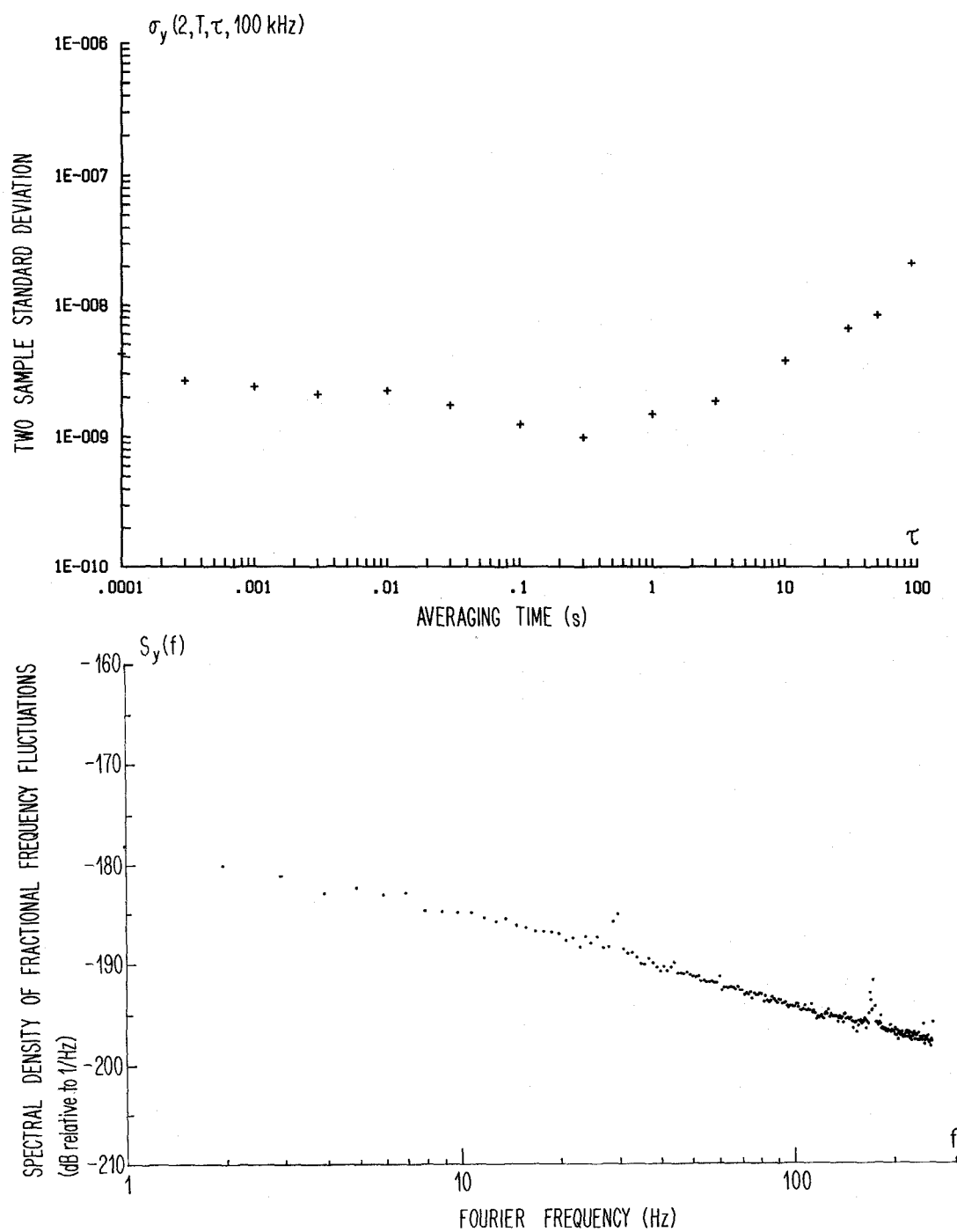
312

Figure 7 - Measurement of short term frequency stability of a cavity-oscillator:

a) time domain measurement: Allan variance;

b) frequency domain measurement: spectral density of the fractional frequency fluctuations.